

T-HISTORY ANALYSIS OF ASPECT RATIO EFFECT ON SUBCOOLING AND SOLIDIFICATION BEHAVIOUR OF PHASE CHANGE MATERIAL IN VERTICAL GLASS TUBES

by

Rudra Murthy B. V. * and Veershetty GUMTAPURE*

Renewable Energy Laboratory, Department of Mechanical Engineering,
National Institute of Technology Karnataka, Surathkal, Mangalore, Karnataka State, India

Original scientific paper
<https://doi.org/10.2298/TSCI200509326M>

The study deals with the effect of the tube aspect ratio on subcooling and the solidification behaviour of phase change material using the T-history method and is compared with the differential scanning calorimetry analysis. Three tubes of different aspect ratios, l/d , and a constant length of 178 mm are chosen for this study. Infrared contour depicts that the inner surface of the glass tube and phase change material initiate heterogeneous nucleation. The differential scanning calorimetry heat flow graph indicates a higher degree of subcooling than T-history method. The study of aspect ratio with and without insulation shows that the mean value of degree of subcooling is less in the insulated tube than non-insulated tube due to reduced cooling rate. The effect of the high aspect ratio is to increase the degree of subcooling due to increased cooling rate and, however, decrease the sensible heat discharge time to reach the plateau, t_{pl} .

Key words: nucleation, latent heat, cooling rate, heat flow, transition temperature, sensible heat

Introduction

Nowadays, phase change materials (PCM) are getting significant attention, owing to store thermal energy in less temperature difference due to their high latent enthalpy. It has a wide range of applications like in energy-efficient buildings for heating and cooling, solar thermal energy storage, electronic device thermal management, medical equipment's, and textiles [1-3]. The PCM should possess desired properties such as a phase change temperature within the working range, a high specific heat, a high thermal conductivity, less or no subcooling, and cost-effective [4]. The study of PCM thermophysical properties is crucial and prime requisite to know the latent heat absorption or phase transition within the application temperature range together with undesired properties like subcooling, incongruent melting, etc. [5, 6]. Subcooling is the effect of cooling a material below its equilibrium melting temperature without becoming solid. When the temperature is low (at any point in a volume), nucleation starts, and the material begins to solidify, called nucleation temperature, for homogeneous nucleation. For heterogeneous nucleation, being started by other substances, e.g., nucleators in the PCM or at container walls, these are relevant. Further nucleation depends on time.

The PCM is existing in the metastable subcooled state below the melting temperature and before the nucleation point. The difference in temperature level between the melting and

* Corresponding authors, e-mail: rudra.me16f13@nitk.edu.in; veersg@nitk.edu.in

nucleation point is the degree of subcooling (DOS). Care should be taken to avoid the subcooling, which affects the storage system [7]. Chen and Lee [8] analyzed the subcooling phenomenon and freezing possibility of water inside horizontal cylinders and reported that the lower the coolant temperature or higher the cooling rate, the greater the chance of subcooling. Further the probability of nucleation was increased by adding nucleating agent into the water. Gunther *et al.* [9] developed an algorithm to study the subcooling for simulating applications with low cooling rates and validated with an experimental study. Taylor *et al.* [10] conducted the experimental characterization of subcooling in inorganic PCM. Found that calcium chloride hex-hydrate salt exhibits a high DOS and pronounced dependency with the cooling rate. Solomon *et al.* [11] studied the various factors affecting the PCM subcooling during the solidification. They reported that subcooling increases with increasing cooling rate and fraction of sensible heat utilized to raise the temperature from nucleation point to solidification point, which effect to reduce the latent heat available for application. Gunther *et al.* [12] performed the experimental study on subcooling in hexadecane emulsion. It was found that emulsion with the smallest droplet size exhibit high DOS and emulsion surfactant significant impact on melting and solidification temperatures.

The T-history method

The T-history method (THM) is a non-commercial and in-house experimental method. Bulk and inhomogeneous PCM samples can be evaluated simultaneously. Zhang *et al.* [13] developed THM in 1999 as a calorimetry method. Marin *et al.* [14] further developed THM by introducing the enthalpy-temperature curve, which is convenient to measure the PCM properties and helps compare with differential scanning calorimetry (DSC). Hong *et al.* [15] improved accuracy by introducing inflection points as the end of the phase transition range. Peck *et al.* [16] proposed the tube placement along the horizontal direction overcome the temperature difference along the vertical direction due to free convection. Tan *et al.* [17] examined the factors that influenced the accuracy and precision of the enthalpy-temperature curve using two diameter tubes with three different thickness insulation. Tube with a high ratio between the thermal mass of the sample to the insulation yield low hysteresis and more precision. Sole *et al.* [18] reviewed the proposed and advance of the THM for the determination of the thermophysical properties of PCM. Even though open literature describes considerable improvement in the THM, there is a lack of significant work on the effect of tube geometry on the subcooling of PCM.

The novelty of this work is to study the effect of aspect ratio on subcooling in THM. The DOS affects the latent enthalpy of the material and requisite property for the proper design of the storage system [7]. It is essential to study the correlation between aspect ratio, cooling rate, sample mass, and subcooling.

Materials and methodology

For this study, commercial PCM OM46 (PLUSS^R) derived from a mixture of organic material has been arbitrarily selected. The data are provided in the certificate of analysis. The OM-46 has desired properties is shown in tab. 1.

Differential scanning calorimetry

Transition temperature and heat flow properties like subcooling of OM-46 is investigated in the dynamic mode DSC apparatus (Mettler Toledo DSC 1 STAR^o System). Temperature and heat-flow calibration is done with indium at the scanning rate of 10 °C per minute. Powdered sample OM-46 is weighed, and the sample is then placed in 40 μ L aluminum crucible

with a pierced lid. This sample is then introduced to a predefined temperature program as to heat and cool the sample at the rate of 2 °C per minute between 0-80 °C. The inert atmosphere has been used for heating and cooling of the sample was done by-passing nitrogen as a purge gas with a flow rate of 20 ml per minute. The sample is retained in an isothermal state for 2 minutes during the start and end of the cycle to achieve the initial steadiness. Isothermal steps help to reduce temperature lag compensation and also improves the results. The STAR[®] S.W. thermal analysis software is used for the evaluation of the heat flow curve.

Table 1. Thermophysical properties of OM-46

Property (solid/liquid)	Value
Melting temperature*	48 °C
Freezing temperature*	45 °C
Latent heat (48-39 °C)*	196 kJ/kg
Specific heat (28 °C/53 °C)*	2.5/2.7 kJ/kgK
Thermal conductivity (5 °C/60 °C)**	0.2/0.1 W/mK
Density (28 °C/55 °C)**	917/880 kg/m ³
Thermal stability**	~2000 cycles
Maximum operating temperature**	120 °C

*Measured data (DSC), ** Manufacturer's nominal data [19]

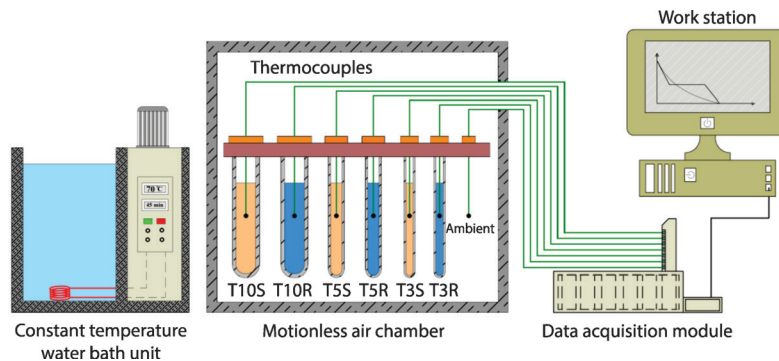


Figure 1. Schematic of in-house T-History experimental set-up with three tubes of different aspect ratios

The T-history method

The scheme of the experimental set-up built in the present work is shown in the fig. 1. Three borosilicate glass tubes (WilmadTM) are shown in fig. 2 of the same length, and different in diameter were used to study the effect of aspect ratio on subcooling in THM. In a cooling experiment, a sample is cooled from the outside. This causes a temperature gradient in the sample. The heat transfer coefficient from the ambience to sample and reference tube is assumed to be the same at that instant and constant over a small interval of time [20].

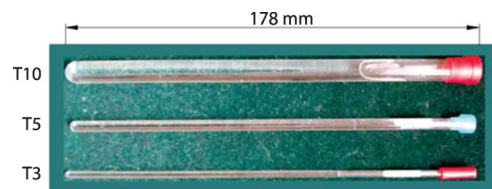


Figure 2. The sample holder of different aspect ratio keeping the length of the tube constant

The heat transfer coefficient from the ambience to sample and reference tube is assumed to be the same at that instant and constant over a small interval of time [20].

The natural-convection heat transfer coefficient of air outside the tube is 4-5 W/m²K [13], and the Biot number eq. (1) for lumped system analysis is evaluated [14]:

$$Bi = \frac{\alpha R}{2\lambda} < 0.1 \quad (1)$$

where R is the inner radius of the sample tube, α – the convective heat transfer coefficient between the tube and the air, and λ – the thermal conductivity of the PCM. The respective values of Biot numbers are tabulated in tab. 2.

The dimension of each glass tube, the mass of the sample, and reference material are listed in tab. 2. All the tubes satisfy the lumped capacity criteria $Bi < 0.1$. The RSTM Pro-calibrated K -type class-I thermocouples of exposed junction and response time are 0.1 second, placed at the center of each sample, and reference tubes. All the thermocouples are calibrated with Pt.100 (RTD) temperature sensors having an accuracy of ± 0.2 °C. O.M. 46 PCM and distilled water are filled in different diameter tubes (T10S, T5S, and T3S) and reference tubes (T10R, T5R, and T3R), respectively.

Constant temperature water bath associated with an 800 W heating capacity possessing accuracy of ± 0.5 °C and temperature regulator manages 5-10 °C temperature range higher than the typical transition temperature of the particular PCM. A motionless air chamber of the thickness of 0.03 m (Styrofoam type) is used to cool the specimen without the disturbance of outside conditions [21]. The provision of heating and cooling of different diameter reference and sample tubes is carried out concurrently to achieve the uniform heating and cooling conditions. Each of the PCM samples, reference, and tubes weighed in analytical balance (Contech^R-CAI 234) of least count 10 mg and are listed in tab. 2. The program is coded in LabVIEW to monitor and acquire the temperature-time data using National InstrumentsTM (NI-cDAQ 9174, NI-9214, and TB-9214) data acquisition system with the sampling rate of 1 Hz.

Table 2. Details of T3, T5, and T10 tube used in THM

Parameters	T10	T5	T3
Outer diameter [mm]*	9.9935 \pm 0.0065	4.97 \pm 0.070	2.99 \pm 0.030
Inner diameter [mm]*	9.070 \pm 0.013	4.20 \pm 0.070	2.41 \pm 0.030
Length [mm]*	178	178	178
Mass of PCM [g]	8.31	1.68	0.55
Mass of reference [g]	9.21	1.8	0.62
Mass of tube [g]	5.44	2.55	1
Aspect ratio (length/inner diameter)	19.6	42.3	73.8
Biot number ($Bi < 0.1$)	0.05	0.02	0.01

*Manufacturers data's

The T-history analysis is carried out in two cases, with and without insulation of the tube. Three repeated trials were performed on all the tubes to check the recurrence and deviation of the results.

Results and discussion

The differential scanning calorimetry

The DSC heat flow curve of PCM OM-46 is shown in fig. 3. The zero slopes of the heat flow curve signify sensible heat absorption and discharge without a phase transition.

However, the instantaneous slope changes to infinite value revealing the latent heat absorption or release at a nearly isothermal state with phase change. Extrapolation onset and the endset temperature is used to identify the melting and solidification range of PCM. The heat flow curve from fig. 3 shows the onset melting point, and the crystallization point is 47.8 °C and 46.2 °C, respectively. However, the corresponding melting and crystallization peaks are observed at 50.2 °C and 45.1 °C, respectively. The DOS evaluated from the DSC heat-flow curve based on the onset-onset approach is 1.6 °C [22].

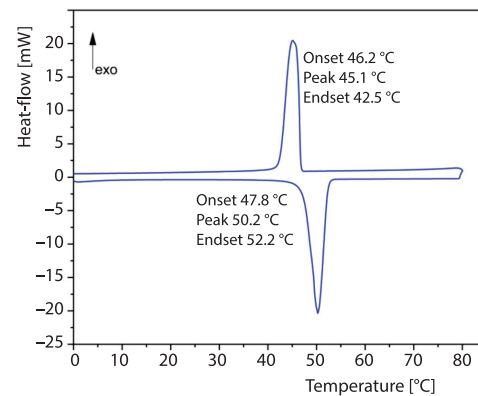


Figure 3. The DSC heat flow graph of OM-46 for heating and cooling run

The T-history cooling infrared image of the sample and reference tubes (T10, T5, and T3) at different time span

The melting contour of all the three tubes at different times are captured using infrared (IR) thermal camera (Testo 865) of accuracy ± 2 °C as shown in fig. 4. The sample (T10S, T5S, and T3S) and reference (T10R, T5R, and T3R) tubes were initially at a thermal equilibrium temperature of 60 °C. The K-type thermocouple is placed at the center of the tubes to monitor the variation of sample and reference temperature with time. The cooling process is divided into three regions: start of the cooling process associated with natural convective motion. The nucleation and phase change process release latent heat and then solidification is dominated by conduction heat transfer.

The IR image captured at the different cooling time indicates the time required for temperature reduction in sensible cooling of PCM before solidification is faster than reference material (distilled water). As the PCM sample undergoes phase change or nucleation, it triggers the latent heat release at almost constant temperature. At this instant, temperature decrement in PCM tubes is lesser than reference tubes as shown in the image captured from 300-2500 seconds. A similar effect is perceived in the temperature-time curve of all three tubes is illustrated in fig. 6. The image captured at 30 seconds indicates that T3R (3 mm reference tube) cools faster than T3S (3 mm sample tube).

Non-uniform temperature is observed (yellow patches at the centre of T3S, fig. 4) even the aspect ratio of T3S tube is very high. However, this indicates that the achievement of the uniform temperature inside the PCM tubes is hypothetical. Due to the density effect of the PCM, the temperature at the top, bottom, and the portion of the PCM which is in contact with the inner surface of the glass tube becomes cold spot as shown in the fig. 4 at a different time interval. It is noticed that in different intervals of IR contour, nucleation triggers form the inner surface of the glass tube towards the center. Because of adhesion force between the PCM and the inner surface of the glass tube, the contraction of PCM upon cooling the cavity has been created inside the tube at the top face of the PCM as shown in the fig. 5. This phenomenon is regarded as heterogeneous nucleation. Nucleation points are triggered near to the inside glass surface releasing the latent heat to subcooled liquid PCM to raise its temperature suddenly from subcooling to the temperature near to the melting point, where the plateau is formed, as shown in fig. 6. The T3 tubes cool faster and reaches the ambient condition as compared to the T5 and T10 due to less material.

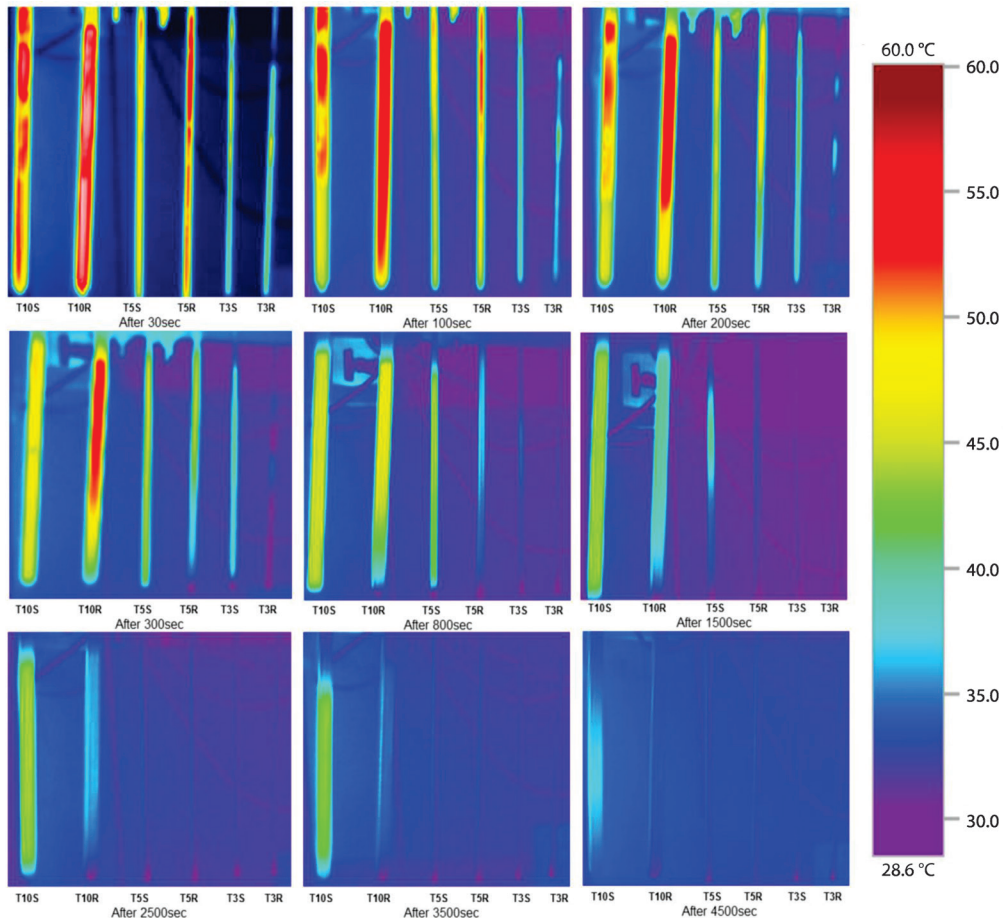


Figure 4. The IR image of T10, T5, and T3 tubes at different cooling time



Figure 5. The PCM cavity formation inside the tube during the cooling process

However, the IR image captured at 800 seconds indicates that T3 sample and reference tubes attain the temperature at lesser than 35 °C. Similar behaviour observed in T5 tube, but the cooling rate T5 tube is lesser than T3 tube due to the higher radius of the tube and more sample material. The T5 reference and sample tubes attain ambient condition, and it is shown in IR image captured at 2500 seconds. The image captured at 4500 seconds indicates T10 tube approaches the ambient conditions.

The T-history cooling without insulation

Three repeated trials had been conducted using tubes of different diameters keeping length the same, *i.e.*, T10, T5, and T3, respectively.

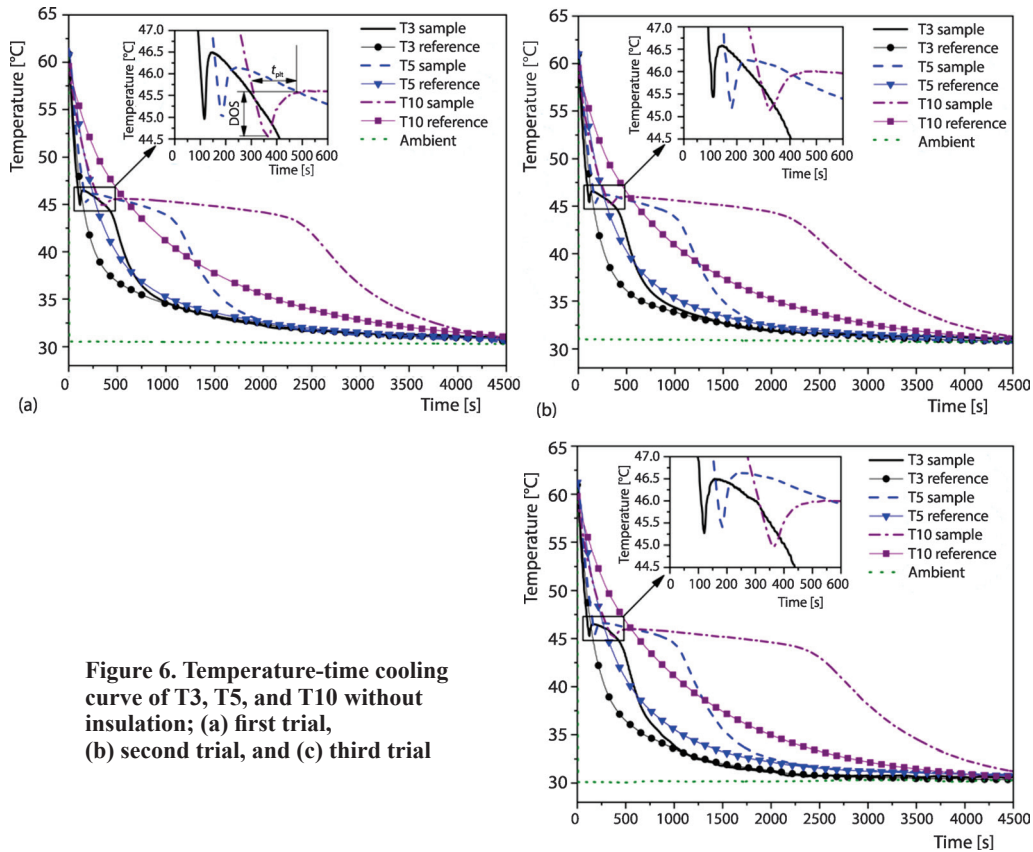


Figure 6. Temperature-time cooling curve of T3, T5, and T10 without insulation; (a) first trial, (b) second trial, and (c) third trial

Table 3. The DOS mean and standard deviation (SD) for T3, T5, and T10 trials without insulation

Tubes	Trials	Nucleation temperature [°C]	Melting temperature [°C]	DOS [°C]	DOS (mean ±SD) [°C]
T3	1 st	44.9	46.5	1.6	1.3 ±0.2
	2 nd	45.3	46.5	1.2	
	3 rd	45.2	46.5	1.3	
T5	1 st	44.9	46.1	1.2	1.1 ±0.1
	2 nd	45.2	46.2	1.0	
	3 rd	45.4	46.6	1.2	
T10	1 st	44.6	45.5	0.9	0.8 ±0.1
	2 nd	45.2	45.9	0.7	
	3 rd	44.9	45.8	0.9	

Heating and cooling for all three tubes were carried out in a similar condition, and observation has been made to study the effect of diameter on subcooling. Even though all the tubes cooled at similar conditions, from fig. 6, the cooling rate of T3 tubes is higher than that of T5 and T10 tubes due to less diameter and sample mass. The average DOS for three trials is more in T3 tube is due to the high cooling rate. However, the heat released from nucleating

points inside the T3 tubes reaches the center of the tube very fast as compared to the T5 and T10 due to less PCM radial thickness between the inner glass surface and the thermocouple point. Hence the period in T3 tube to raise its temperature from the sub-cooling point to the melting point plateau is very less. This factor is evident from the temperature-time curve obtained for all the three repeated trials and is shown in fig. 6. The DOS for the individual trials of all three tubes and its average value is listed in tab. 3.

The T-history cooling with one layer of insulation

To study the effect of cooling rate on subcooling, T3, T5, and T10 tubes were provided with one layer of nitrile foam insulation of thickness 3 mm and the trials are repeated with the similar cooling condition as considered for the tubes without insulation case. In THM, three cooling trial data of all three tubes were obtained and are plotted as shown in fig. 7.

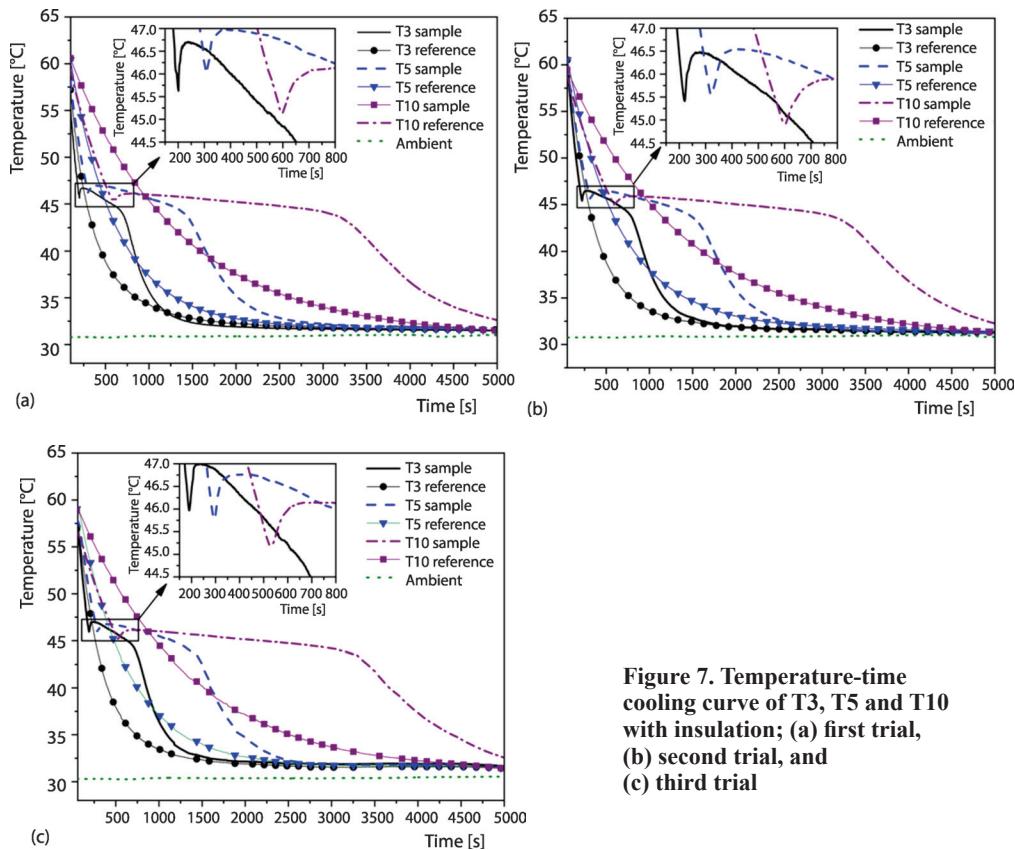


Figure 7. Temperature-time cooling curve of T3, T5 and T10 with insulation; (a) first trial, (b) second trial, and (c) third trial

The quantitative values obtained from the T-history cooling curve, *i.e.*, nucleation point, melting temperature, and DOS of three trials, are tabulated in tab. 4. From the calculated average and SD values, it is observed that DOS is in the order of $T3 > T5 > T10$.

Comparison of DOS with and without insulation

Quantitative comparison of DOS values in tabs. 3 and 4 yields that DOS is less in all insulated tubes indicating that the provision of insulation reduces the cooling rate, and the reduction in the DOS value proves the relation, eq. (2). The hypothetical DOS triangle is shown

in fig. 8, where the height and base of the triangle indicate DOS and time to reach a plateau, t_{pit} , respectively. From figs. 6 and 7, it is observed that the DOS is increasing with an increase in the aspect ratio (i.e., $T3 > T5 > T10$). However, the t_{pit} is decreasing with an increase in the aspect ratio (i.e., $T3 < T5 < T10$). From the analysis of tubes with one layer of insulation, a reduction is noticed in DOS as compared with the respective tubes without insulation.

Table 4. The DOS mean and SD for T3, T5, and T10 trials with insulation

Tubes	Trials	Nucleation temperature [°C]	Melting temperature [°C]	DOS [°C]	DOS (mean ±SD) [°C]
T3	1 st	45.6	46.6	1	1 ±0.1
	2 nd	45.4	46.3	0.9	
	3 rd	45.9	47	1.1	
T5	1 st	46	47	1	0.8 ±0.15
	2 nd	45.7	46.4	0.7	
	3 rd	45.9	46.7	0.6	
T10	1 st	45.1	45.6	0.5	0.6 ±0.1
	2 nd	44.8	45.5	0.7	
	3 rd	45.2	45.8	0.6	

$$\left(\frac{dT}{dt}\right)_{cooling} \propto DOS \quad (2)$$

However, the t_{pit} has no considerable changes noticed between insulated and non-insulated tubes during a similar cooling condition. In insulated tubes, heat exchange is controlled between PCM and ambient as compared with the non-insulated tubes. The insulated tube facilitates more sensible heat transfer from nucleation sites to the PCM around the thermocouple. However, it proves that insulation affects the cooling rate (dT/dt) only. Neither it affects the nucleation progress nor the release of sensible heat at the nucleation site to reach the plateau or melting point, t_{pit} . Due to more sample mass in higher diameter tube, heterogeneous nucleation triggers at the inner surface of the glass tube take more time to reach the released sensible heat towards the tube center where the thermocouple is placed. So discharge time or time required to attain a plateau, t_{pit} , is more in higher diameter tubes, eq. (3). Therefore:

$$d_t \text{ or } m_p \propto t_{pit} \quad (3)$$

where d_t is the tube diameter, m_p – the sample mass (PCM), and t_{pit} – the time required to reach plateau or melting point.

Conclusions

In the present study, the effect of aspect ratio on the subcooling of the PCM OM46 is considered as a potential material for the medium temperature application based on nominal melting temperature. The following conclusions are made from the present DSC result and T-history analysis with three different aspect ratio tubes as follows.

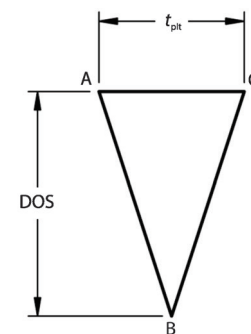


Figure 8. The DOS triangle

- The DOS is more in the DSC heat flow curve due to a higher cooling rate and lesser sample mass than the T-history analysis.
- The IR contour at different cooling times show that T3 sample tube cools faster at a nearly uniform temperature. Nucleation triggers between the inner surface of the glass tube and the PCM is due to the adhesion force and is termed as heterogeneous nucleation.
- As the diameter of the tube decreases or aspect ratio increase, cooling rate increases, which in turn affects the high DOS value.
- The T-history cooling with tube insulation reduces the heat transfer from tube to the ambient, *i.e.*, reducing the cooling rate and lowers the DOS.
- The increased diameter or the sample mass effects the sensible heat discharge time, t_{plt} , to attain plateau (melting temperature). However, the reduction in speed of solidification reduces the temperature level of the plateau. Because of a large fraction of sample mass below melting temperature, this absorbs more latent heat released by the nucleating site to increase the temperature of the PCM. This results in the reduction of the latent heat released by the PCM.
- For the accurate determination of transition temperature and latent enthalpy of PCM in THM, it is recommended to use high aspect ratio tubes owing to nearly uniform temperature inside the PCM. However, high aspect ratio tubes take less t_{plt} . In addition, choosing the lower cooling rate leads to a significant reduction in DOS.

References

- [1] Zhou, D., *et al.*, Review on Thermal Energy Storage with Phase Change Materials (PCM) in Building Applications, *Applied Energy*, 92 (2012), Apr., pp. 593-605
- [2] Yang, L., *et al.*, Thermophysical Properties and Applications of Nanoenhanced PCM: An Update Review, *Energy Conversion and Management*, 214 (2020), June, 112876
- [3] Fokaides, P. A., *et al.*, Phase Change Materials (PCM) Integrated into Transparent Building Elements: A Review, *Materials for Renewable and Sustainable Energy*, 4, (2015), Apr., 6
- [4] Mehling, H., Cabeza, L. F., Phase Change Materials and Their Basic Properties, in: *Thermal Energy Storage for Sustainable Energy Consumption*, (ed. Paksoy H. O.), NATO Science Series (Mathematics, Physics and Chemistry), Vol 234. Springer, Dordrecht, Germany, 2007
- [5] Wei, G., *et al.*, Selection Principles and Thermophysical Properties of High Temperature Phase Change Materials for Thermal Energy Storage, A Review, *Renewable and Sustainable Energy Reviews*, 81 (2018), Part 2, pp. 1771-1786
- [6] Atinafu, D. G., *et al.*, Thermal Properties of Composite Organic Phase Change Materials (PCMs): A Critical Review on Their Engineering Chemistry, *Applied Thermal Engineering*, 181 (2020), Nov., 115960
- [7] Mehling H, Cabeza, L. F., *Heat and Cold Storage with PCM, An Up to Date Introduction into Basics and Applications*, Springer, New York, USA, 2008
- [8] Chen, S. L., Lee, T. S., A Study of Supercooling Phenomenon and Freezing Probability of Water Inside Horizontal Cylinders, *Int. J. Heat Mass Transf.*, 41 (1998), 4-5, pp. 769-783
- [9] Gunther, E., *et al.*, Modelling of Subcooling and Solidification of Phase Change Materials, *Model. Simul. Mater. Sci. Eng.*, 15 (2007), 8, pp. 879-892
- [10] Taylor, R. A., *et al.*, Experimental Characterisation of Sub-Cooling in Hydrated Salt Phase Change Materials, *Appl. Therm. Eng.*, 93 (2016), C, pp. 935-938
- [11] Solomon, G. R., *et al.*, Sub Cooling of PCM Due to Various Effects during Solidification in a Vertical Concentric Tube Thermal Storage Unit, *Appl. Therm. Eng.*, 52 (2013), 2, pp. 505-511
- [12] Gunther, E., *et al.*, Subcooling in Hexadecane Emulsions, *Int. J. Refrig.*, 33 (2010), 8, pp. 1605-1611
- [13] Zang, Y., *et al.*, A Simple Method, the T-History Method, of Determining the Heat of Fusion, Specific Heat and Thermal Conductivity of Phase-Change Materials, *Meas. Sci. Technol.*, 10 (1999), 3, pp. 201-205
- [14] Marin, J. M., *et al.*, Determination of Enthalpy-Temperature Curves of Phase Change Materials with the Temperature-History Method: Improvement to Temperature Dependent Properties, *Meas. Sci. Technol.*, 14 (2003), 2, pp. 184-189
- [15] Hong, H., *et al.*, Accuracy Improvement of T-History Method for Measuring Heat of Fusion of Various Materials, *Int. J. Refrig.*, 27 (2004), 4, pp. 360-366

- [16] Peck, J. H., A Study of Accurate Latent Heat Measurement for a PCM with a Low Melting Temperature Using T-History Method, *Int. J. Refrig.*, 29 (2006), 7, pp. 1225-1232
- [17] Tan, P., *et al.*, Characterizing Phase Change Materials Using the T-History Method: On the Factors Influencing the Accuracy and Precision of the Enthalpy-Temperature Curve, *Thermochim. Acta.*, 666 (2018), Aug., pp. 212-228
- [18] Sole , A., *et al.*, Review of the T-History Method to Determine Thermophysical Properties of Phase Change Materials (PCM), *Renewable and Sustainable Energy Reviews*, 26 (2013), Oct., pp. 425-436
- [19] ***, PLUSSR India, Technical data sheet of the manufacturer <https://www.pluss.co.in/product-range-PCM.php>, 2019
- [20] Badenhorst, H., Cabeza, L. F., Critical Analysis of the T-History Method: A Fundamental Approach, *Thermochim. Acta.*, 650 (2017), Apr., pp. 95-105
- [21] Rudra Murthy, B. V., Gumtapure, V., Thermal Property Study of Fatty Acid Mixture as Biophase Change Material for Solar Thermal Energy Storage Usage in Domestic Hot Water Application, *Journal Energy Storage*, 25 (2019), Aug., 100870
- [22] ***, Wiki PCM, Approaches to determine the values of supercooling. <https://thermalmaterials.org/wiki-pcm/supercooling>, 2019